

SEGMENTATION OF MITOCHONDRIA IN ELECTRON MICROSCOPY IMAGES USING ALGEBRAIC CURVES

Mojtaba Seyedhosseini¹, Mark H. Ellisman², Tolga Tasdizen¹

¹Scientific Computing and Imaging Institute, University of Utah

²National Center for Microscopy and Imaging Research, University of California, San Diego

ABSTRACT

High-resolution microscopy techniques have been used to generate large volumes of data with enough details for understanding the complex structure of the nervous system. However, automatic techniques are required to segment cells and intracellular structures in these multi-terabyte datasets and make anatomical analysis possible on a large scale. We propose a fully automated method that exploits both shape information and regional statistics to segment irregularly shaped intracellular structures such as mitochondria in electron microscopy (EM) images. The main idea is to use algebraic curves to extract shape features together with texture features from image patches. Then, these powerful features are used to learn a random forest classifier, which can predict mitochondria locations precisely. Finally, the algebraic curves together with regional information are used to segment the mitochondria at the predicted locations. We demonstrate that our method outperforms the state-of-the-art algorithms in segmentation of mitochondria in EM images.

Index Terms— Mitochondria segmentation, algebraic curves, random forest, electron microscopy imaging

1. INTRODUCTION

The morphology and distribution of intracellular components are of substantial biological importance for neuroscientists. For example, abnormal mitochondria morphology can be seen in Parkinson’s disease-related genes [5] or geometrical properties of mitochondria can be used to distinguish cancer cells from normal cells [13]. In addition, an accurate mitochondria segmentation would improve cell segmentation results by distinguishing mitochondria membranes from other cell membranes [7]. Electron microscopy (EM) imaging techniques generate nanoscale images that contain enough details

for study of intracellular components, such as mitochondria. However, the sheer size of a typical EM dataset, often approaching tens of terabytes [1], makes manual analysis infeasible [3]. Hence, automated image analysis is required. However, fully automatic analysis is challenging because numerous intracellular components exhibit irregular shapes and have similar local appearances [12]. Moreover, the texture and physical topologies of intracellular components are highly variable [9] (Figure 1). A robust automated segmentation method must overcome these issues.

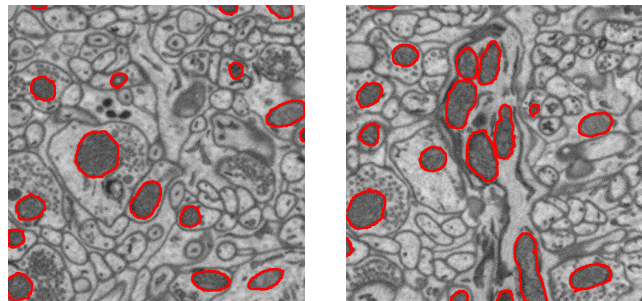


Fig. 1. Mitochondria (red outlines) appear in different shapes and intensities in EM images. This variety and the existence of other similar structures make segmentation a difficult task.

General segmentation methods which have been proposed for natural image datasets yield poor results when applied to EM images [12]. Jain et.al. [8] showed that global probability boundary [2] and boosted edge learning [6], which result in outstanding segmentation performance on natural images, perform poorly on EM datasets. Therefore, a successful method for segmenting specific structures such as mitochondria must be optimized for EM images.

There are several segmentation methods that handle EM images specifically. In [18], a graph-cut method is proposed that minimizes an energy function over the pixel intensity and flux of the gradient field for cell segmentation. However, this model might be confused by the complex intracellular structures. In [17], textural information is used to train a Gentleboost classifier for mitochondria segmentation of the lateral part of the rat’s brain. In [13], texton-based region features are used with different classification methods to segment mi-

This work was supported by NIH 1R01NS075314-01 (TT,MHE) and NSF IIS-1149299 (TT). The microscopy studies producing data for these developments were carried out at the National Center for Microscopy and Imaging Research at UCSD supported by an award from NIH NCRR (P41 GM103412) to MHE. The image data for these projects are available for open access from the Cell Image Library/Cell Centered Database supported by grants from the NIH NIGMS (R01 GM082949) to MHE and Maryann Martone.

tochondria in MNT-1 cells. Even though these methods make extensive use of textural information, they ignore the shape information. In [14], Ray features are proposed to capture shape information for detection of irregular shapes such as mitochondria. But, they only rely on geometric information of shapes and ignore texture information. Radon like features [10] are another set of features designed to take both texture and geometric information into account and can be tuned to segment different objects in EM images.

More powerful mitochondria segmentation methods working on 3D volumes have been proposed recently. Lucchi et.al. [11] solved a graph partitioning problem by learning a classifier based on the textural and shape information to segment mitochondria. Giuly et.al. [7] proposed a multi-step approach that exploits a patch classifier followed by a contour pair classification and level sets. We also propose a multi-step approach that combines textural and shape information to provide a high-accuracy mitochondria segmentation. As a first step, we extract patches with different sizes from the input image and fit algebraic curves, of different degrees, to each patch. Next, shape and texture features are extracted based on the fitted polynomials. These features are then used to train a classifier that predicts if a patch belongs to mitochondria. Finally, in the patches containing mitochondria, based on the classifier decision, we use the connected component of the center pixel bounded by the fitted polynomial to segment the mitochondria.

Algebraic curves, i.e., the zero level set of polynomials in two variables, are suitable for modelling complicated shapes [16]. Moreover, they take advantage of all data in an image patch and thus are able to find weak edges embedded in noise [15]. We take advantage of the power of algebraic curves in finding ambiguous edges in cluttered backgrounds to estimate the boundary of mitochondria and extract informative shape and textural features from images. The regional features, i.e., textural features from image regions, are more robust and informative compared to pixel features.

2. METHOD

Our proposed method is composed of four steps: Curve fitting, feature extraction, detection, and pixel labelling.

2.1. Curve fitting

A d th degree polynomial can be represented by $f_d(x, y) = \sum_{0 \leq l+m \leq d} a_{lm} x^l y^m$. Given an $n \times n$ image patch $P(x, y)$, we fit a polynomial to the patch by minimizing the cost function E :

$$E = \sum_{i,j=1}^n w_{ij}^2 (f_d^2(x_i, y_j) + (\frac{\nabla P(x_i, y_j)}{w_{ij}} \cdot \nabla f_d(x_i, y_j) - 1)^2) \quad (1)$$

where $\nabla P(x_i, y_j)$ denotes the gradient vector at pixel (x_i, y_j) , $\nabla f_d(x_i, y_j)$ is the gradient vector of polynomial f at (x_i, y_j) ,

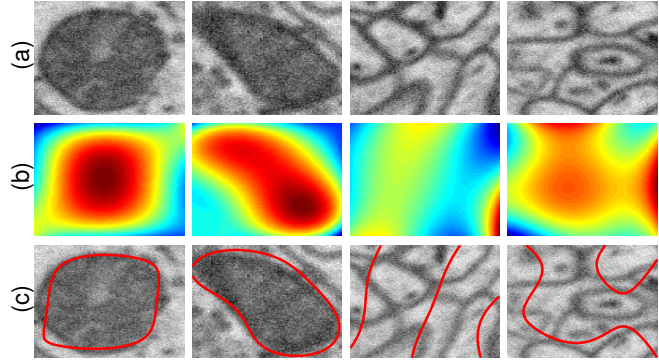


Fig. 2. (a) Two patches with mitochondria (two left columns) and two patches without mitochondria (two right columns) in them, (b) fitted polynomials of degree 4 to the patches in (a), and (c) the zero level sets overlaid on the input patches.

and w_{ij} is the length of $\nabla P(x_i, y_j)$. This minimization problem can be solved using linear least squares [15].

In Eq. 1, the $f_d^2(x_i, y_j)$ term determines the zero level set of the fitted polynomial, i.e., $f_d(x, y) = 0$, and the $(\frac{\nabla P(x_i, y_j)}{w_{ij}} \cdot \nabla f_d(x_i, y_j) - 1)^2$ term forces the $\nabla f_d(x, y)$ to have the same direction as $\nabla P(x, y)$ with unit magnitude at each point. The effect of large gradients in noisy areas is damped by this unit magnitude constraint. Finally, the w_{ij}^2 term increases the influence of pixels with large gradient magnitude. These pixels are most likely on the target contour and have larger gradient magnitudes compared to noisy pixels. The above-mentioned properties make this fitting strategy appropriate for noisy EM images with complex regional textures. In addition, this fitting strategy is rotation and scale invariant and thus is suitable for shape representation. Figure 2 shows the fitted polynomials to two patches with mitochondria and two patches without mitochondria in them.

2.2. Feature extraction

We use zero level sets of the fitted polynomials (Figure 2(c)) to extract both shape and textural features from each patch. The zero level set divides each patch to two disjoint regions: inside, i.e., $f_d(x, y) > 0$ and outside, i.e., $f_d(x, y) < 0$. Each polynomial thus forms a hypothesis of existence of a mitochondrion in the patch. The inside region and the zero level set curve exhibit similar features among the patches with mitochondria (two left columns in Figure 2) which are different from features of the patches without mitochondria (two right columns in Figure 2). The textural features are extracted from inside of the zero level set curve and include Hu's invariant moments, mean, variance, skewness, kurtosis, and entropy of the pixel intensities. The shape features are extracted from the zero level set curve itself. They contain Hu's invariant moments of the curve and the average intensity of pixels on the curve. We also use the ratio of the inner area to the curve length as another shape feature. The combination of the tex-

tural and shape features provide a rich set of features that can be used to detect mitochondria in an image.

2.3. Detection

The extracted features from each patch are used to train a binary random forest classifier that predicts whether that patch belongs to a mitochondrion or not. In practice, we extract many patches with different sizes at different locations and fit polynomials of different degrees to each of them. It is worth noting that we use different patch sizes due to different sizes of mitochondria and fit polynomials of different degree due to different shape complexities of mitochondria. The shape and textural features are then extracted from each patch. To train the classifier, the patches that their centers are close to centers of mitochondria are considered as positive samples and the remaining patches are considered as negative samples. The centers of mitochondria are the center of mass of connected components in groundtruth images. The classifier indeed tests the hypothesis that made by the polynomials. It must be emphasized that many of them will be false because there are few mitochondria in each image.

2.4. Pixel labelling

For a given input image, overlapping patches with different sizes are extracted. Next, polynomials of different degrees are fitted to each patch and the shape and textural features are computed for each patch. These features are then passed to the random forest classifier. If a patch is classified as positive by the random forest classifier, all the connected pixels of the center pixel in that patch are marked as mitochondria in the input image. The connected pixels of the center pixel are found in a certain threshold around the intensity of the center pixel. To add more certainty to the labelling process, we only mark the connected pixels inside the zero level set as mitochondria and consider the remaining pixels as background.

The segmentation accuracy can be improved by applying morphological post-processing. We apply the morphological dilation followed by the region filling to fill holes in the segmented mitochondria.

3. RESULTS AND CONCLUSION

We test the performance of our proposed method on two different sets of EM images: mouse neuropil and *Drosophila* ventral nerve cord (VNC) [4]. The mouse neuropil dataset contains 40 images of size 700×700 . 14 of these images were used for training and the remaining images were used for testing. The *Drosophila* VNC dataset contains 30 images of size 512×512 . 15 of these images were used for training and the remaining images were used for testing. The groundtruth images of mitochondria were annotated by a neuroanatomist.

For both of the datasets, we extracted patches with four different sizes, 48×48 , 64×64 , 88×88 , 104×104 , and fit

Table 1. Testing performance of different methods for the mouse neuropil dataset.

Method	Precision	Recall	Fvalue
Pixel classifier	67.18%	68.05%	67.61%
RLF [10]	78.07%	82.31%	80.14%
Proposed method	82.51%	82.47%	82.49%

polynomials of two different degrees, 2 and 4. The discussed features in section 2.2 were then extracted and a random forest classifier with 100 trees was trained.

We compared the accuracy of our proposed method with a patch-based pixel classifier and the radon-like features method [10]. An artificial neural networks classifier with 10 hidden nodes was used as the pixel classifier. For both of the pixel classifier and RLF method, the best threshold was found using the training results. Table 1 shows the segmentation accuracy of different methods for the testing set in the mouse neuropil dataset. It can be observed that our proposed method has better performance than the other two methods; a 14.9% and 2.4% improvement in the testing F-value compared to the pixel classifier and the RLF method respectively.

For the *Drosophila* VNC dataset, we compared our proposed method with Giuly et.al. [7] method ¹ in addition to the pixel classifier and the RLF method. This dataset is more difficult and the quality of images is lower than the mouse neuropil dataset. While the performance of RLF method was close to the performance of our proposed method for the mouse neuropil dataset, our method outperformed the RLF method with more than 20% in the testing F-value for this dataset. One of the advantages of our method is that it is robust against the texture and noise in the EM images and thus performs reasonably well even for low quality datasets like *Drosophila* VNC dataset. The segmentation accuracy results are shown in Table 2. The segmentation results of mitochondria for two test images from the mouse neuropil and the *Drosophila* VNC dataset are shown in Figure 3.

Table 2. Testing performance of different methods for the *Drosophila* VNC dataset.

Method	Precision	Recall	Fvalue
Pixel classifier	31.29%	60.44%	41.24%
RLF [10]	46.12%	57.67%	51.25%
Giuly et.al. [7]	64.22%	57.01%	60.40%
Proposed method	78.57%	68.08%	72.95%

Conclusion: This paper introduced a mitochondria segmentation framework using algebraic curves. The main idea

¹The results of Giuly et.al. [7] method was only available for the *Drosophila* VNC dataset. We thank Richard J. Giuly for providing these results.

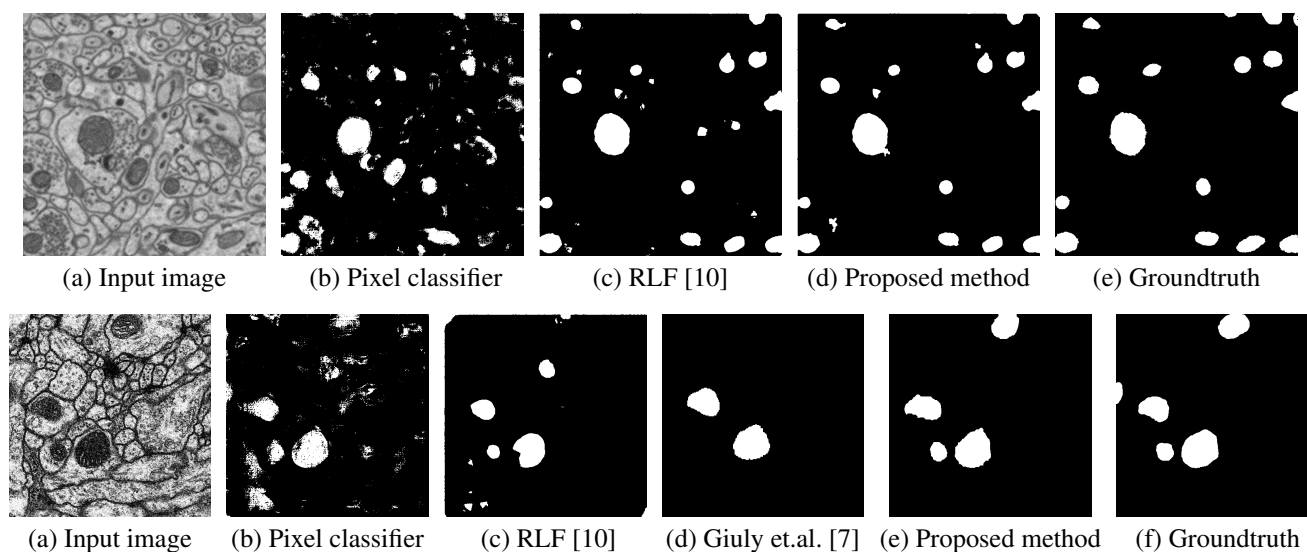


Fig. 3. Test results for the mitochondria segmentation. First row: mouse neuropil dataset, second row: *Drosophila* VNC dataset.

of our method is to use the power of algebraic curves to extract both shape and textural features from input images. The algebraic curves use all the information in a window and are robust against noise and texture. Moreover, algebraic curves enable our method to use regional features that are more informative compared to pixel-wise features. We use the extracted feature to train a random forest which detects mitochondria in input images. Finally, we apply an automatic pixel labelling approach by finding connected components of the center pixels in the patches that the classifier classifies them as positive samples.

4. REFERENCES

- [1] J. Anderson, B. Jones, C. Watt, M. Shaw, J.-H. Yang, D. DeMill, J. Lauritzen, Y. Lin, K. Rapp, D. Mastronarde, P. Koshevoy, B. Grimm, T. Tasdizen, R. Whitaker, and R. Marc. Exploring the retinal connectome. *Molecular Vision*, (17):355–379, 2011.
- [2] P. Arbelaez, M. Maire, C. Fowlkes, and J. Malik. From contours to regions: An empirical evaluation. *CVPR*, 0:2294–2301, 2009.
- [3] K. L. Briggman and W. Denk. Towards neural circuit reconstruction with volume electron microscopy techniques. *Curr. Opin. in Neurobio.*, 16(5):562–570, 2006.
- [4] A. Cardona, S. Saalfeld, J. Schindelin, I. Arganda-Carreras, S. Preibisch, M. Longair, P. Tomancak, V. Hartenstein, and R. J. Douglas. Trakem2 software for neural circuit reconstruction. *PLoS ONE*, 7(6):e38011, 06 2012.
- [5] D. Cho, T. Nakamura, and S. Lipton. Mitochondrial dynamics in cell death and neurodegeneration. *Cellular and Molecular Life Sciences*, 67(20):3435–3447, 2010.
- [6] P. Dollar, Z. Tu, and S. Belongie. Supervised learning of edges and object boundaries. *CVPR*, 2006.
- [7] R. Giuly, M. Martone, and M. Ellisman. Method: automatic segmentation of mitochondria utilizing patch classification, contour pair classification, and automatically seeded level sets. *BMC Bioinformatics*, 13(1):29, 2012.
- [8] V. Jain, B. Bollmann, M. Richardson, D. Berger, M. Helmstaedter, K. Briggman, W. Denk, J. Bowden, J. Mendenhall, W. Abraham, K. Harris, N. Kasthuri, K. Hayworth, R. Schalek, J. Tapia, J. Lichtman, and H. Seung. Boundary learning by optimization with topological constraints. *CVPR*, pages 2488–2495, 2010.
- [9] V. Jain, J. F. Murray, F. Roth, S. Turaga, V. Zhigulin, K. L. Briggman, M. N. Helmstaedter, W. Denk, and H. S. Seung. Supervised learning of image restoration with convolutional networks. *ICCV*, pages 1–8, 2007.
- [10] R. Kumar, A. Va andzquez Reina, and H. Pfister. Radon-like features and their application to connectomics. In *CVPRW*, pages 186–193, 2010.
- [11] A. Lucchi, K. Smith, R. Achanta, G. Knott, and P. Fua. Supervoxel-based segmentation of mitochondria in em image stacks with learned shape features. *IEEE Tran. on Medical Imaging*, 31(2):474–486, 2012.
- [12] A. Lucchi, K. Smith, R. Achanta, V. Lepetit, and P. Fua. A fully automated approach to segmentation of irregularly shaped cellular structures in em images. In *MICCAI (2)*, pages 463–471, 2010.
- [13] R. Narasimha, H. Ouyang, A. Gray, S. W. McLaughlin, and S. Subramaniam. Automatic joint classification and segmentation of whole cell 3d images. *Pattern Recogn.*, 42(6):1067–1079, 2009.
- [14] K. Smith, A. Carleton, and V. Lepetit. Fast ray features for learning irregular shapes. *ICCV*, 2009.
- [15] T. Tasdizen and D. B. Cooper. Boundary estimation from intensity/color images with algebraic curve models. *ICPR*, 1:225–228, 2000.
- [16] T. Tasdizen, J. P. Tarel, and D. B. Cooper. Algebraic curves that work better. *CVPR*, 2:35–41, 1999.

- [17] S. Vitaladevuni, Y. Mishchenko, A. Genkin, D. Chklovskii, and K. Harris. Mitochondria detection in electron microscopy images. *Workshop Microscopic Image Anal. Appl. Biol*, 2008.
- [18] N. Vu and B. S. Manjunath. Graph cut segmentation of neuronal structures from transmission electron micrographs. In *ICIP*, pages 725–728, 2008.